

Topological Defects and the Optimum Size of DNA Condensates

Stella Y. Park,* Daniel Harries,# and William M. Gelbart*

*Department of Chemistry and Biochemistry, University of California, Los Angeles, California 90095-1569 USA, and #Department of Physical Chemistry and The Fritz Haber Research Center, The Hebrew University of Jerusalem, Jerusalem 91904, Israel

ABSTRACT Under a wide variety of conditions, the addition of condensing agents to dilute solutions of random-coil DNA gives rise to highly compact particles that are toroidal in shape. The size of these condensates is remarkably constant and is largely independent of DNA molecular weight and basepair sequence, and of the nature of condensing agent (e.g., multivalent cation, polymers, or added cosolvent). We show how this optimum size is determined by the interactions between topological defects, which unavoidably strain the circumferentially wound DNA strands in the torus.

INTRODUCTION

In many biological processes, intrinsic bias and redundancy aid in accomplishing what at first glance may seem an impossible feat. The packaging of DNA into a condensed state within both prokaryotic and eukaryotic cells may be such a process. It has been known for some time that “naked” DNA undergoes a dramatic compaction in the presence of various condensing agents, mainly multivalent cations, neutral and charged polymers, and alcohols (for recent reviews, see Bloomfield, 1991 and 1996, and references therein). Even in the very dilute regime (well below the bulk phase separation concentration), random-coil DNA molecules condense either intramolecularly (collapse) or intermolecularly (aggregation) to form toroids and rods of a certain size. It is the condensation of DNA in this very dilute regime, not the bulk DNA condensation (Durand et al., 1992), which we discuss in this paper. The highly ordered condensates occupy $\sim 10^{-4}$ the volume of the random coils. The local concentration of DNA within the torus is as large as 400 mg/ml (0.4 g/cm³). (Note that the bulk concentration of DNA in these very dilute solutions can be as small as μ g/ml.) Self-assembly processes involving collapse and aggregation are not only observed in vitro, but are also implicated in the organization/compaction of DNA inside the cell nucleus, where a broad variety of condensing agents—both histone (Ramakrishnan, 1997; Kornberg and Lorch, 1992) and nonhistone (Lepault et al., 1987; Lerman, 1974; Livolant, 1984)—are present.

Electron microscopy provides strong evidence for circumferential winding of DNA within the toroidal condensates. Marx and Ruben (1983) have shown via freeze-etch studies that their spermidine-condensed DNA toroids are indeed circumferentially wound. Other experimental techniques, such as x-ray diffraction (Maniatis et al., 1974), provide data consistent with local hexagonal ordering of

DNA strands (in polymer-and-salt-induced (or Ψ)-condensed DNA) having interaxial spacings of 25–30 Å (see Fig. 1). All of these structural data apply to both intra(mono)-molecular and inter(multi)-molecular condensation of DNA in dilute solutions, and highlight the high degree of organization within the toroids.

Still more remarkable is the fact that the size of the condensates appears to be largely independent of all of the following: the molecular weight of DNA; genetic information (base pair sequence of DNA); the condensing agent used; and the background salt concentrations! More explicitly, over a wide range of DNA lengths (400–50,000 bp), the size (and therefore the number of base pairs—about 50,000) of the torus remains invariant for DNA samples from many different sources and for a wide variety of condensing agents. It is this special condensate size whose existence we propose to explain in the present work.

Until now, it has been the shape of toroidal condensates that attracted most of the theoretical attention. Here, the toroidal aspect ratio—the cross-sectional radius, b , to the toroidal radius, R (see Fig. 1)—determines the shape of the torus. The rod-like condensate, which we do not take into consideration here, has a rod aspect ratio $\approx (1/2\pi) \cdot$ (toroidal aspect ratio) in the same solvent. For example, Ubbink and Odijk (1995) have recently proposed a model for Ψ -toroidal condensates in which they quantitatively analyze the optimal toroidal shape for monomolecular collapse. The size of the condensates is therefore simply dependent on the length (molecular weight) of the chain considered. The same authors have also studied nonideal (noncircular cross section) toroids (Ubbink and Odijk, 1996). Likewise, Grosberg and Zhestkov (1986) and Vasilevskaya et al. (1997) have also studied the DNA monomolecular collapse as a coil-globule transition. Both groups present phase diagrams as a function of DNA molecular weight. They determined the maximum length of DNA that would form toroidal condensates; beyond this length they propose that spherical globules are dominant. This is in qualitative agreement with the experimental findings that both toroids (Yoshikawa et al., 1996; Laemmli, 1975) and spherical globules (Vasilevskaya et al., 1997) are observed for T4 “giant” DNA (166,000 bp).

Received for publication 17 November 1997 and in final form 20 April 1998.

Address reprint requests to Stella Y. Park, Department of Chemistry and Biochemistry, University of California, Los Angeles, CA 90095-1569. Tel.: 310-206-2330; Fax: 310-206-4038; E-mail: parks@chem.ucla.edu.

© 1998 by the Biophysical Society

0006-3495/98/08/714/07 \$2.00

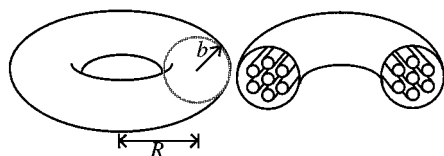


FIGURE 1 A circular torus and a cross-sectional view of circumferentially wound strands.

It is also known that DNA molecules much shorter than 400 bp (e.g., 140 bp; Widom and Baldwin, 1980) will not form toroids. A plausible explanation was presented by Manning (1985). DNA bending was modeled as a series of kinks with a certain kink angle and segment length (over which the strand is straight). In this purely mechanical model, a length was found beyond which buckling—associated with toroid formation—can be observed for a given ionic strength. For example, at a salt concentration of $\sim 10^{-3}$ M, this critical buckling length was ~ 350 Å (100 bp). Alternatively, a kinetic model has been proposed by Hud et al. (1995) in which the dynamics of loop formation determine the toroidal shape. Their loop formation probability and free energy change must be related to the nucleation rate and free energy change proposed for 60-bp segment loops (Manning, 1980).

Our aim is different from the goals of the previous theories; we are specifically interested in the size of the DNA condensates and its apparent insensitivity to molecular weight. This phenomenon is somewhat reminiscent of the micellization of amphiphilic molecules (see, for example, Ben-Shaul and Gelbart, 1994) and of the single-polymer coil-globule transition (see, for example, Lifshitz et al., 1978; Post and Zimm, 1979). As with micelles, the size of the condensates may be a result of competition between surface energy and dispersional entropy. And the uniform, high density of DNA within the torus is suggestive of a macromolecular globule. But, unlike micelles, where the molecular length scale constrains the spherical radius, the rod diameter, or the bilayer thickness, and unlike the coil-globule transition, where $R_{\text{globule}} \propto \text{contour length}^{1/3}$, neither the diameter of the double helix nor its molecular weight fixes either of the toroidal dimensions. Both the micellization and coil-globule situations involve a single length (structure) variable. Conversely, in the current problem, a toroidal DNA condensate can increase its volume upon the addition of monomers (bp's) by increasing either its cross-sectional area or its radius (b^2 and R , respectively, in Fig. 1). Here, then, there are two variables involved, and consequently there is no obvious basis for the preferred size of the toroidal condensate.

In this paper, we represent DNA as a flexible rod (“garden hose”) in which the primary (bp sequence) and secondary (double helix) structures are ignored. Continuing the metaphor, imagine that a garden hose is wrapped around itself or around a cylinder. It is immediately apparent that crossovers—nonparallel portions—of strands are necessary

to “compact” the hose. These are topologically necessary defects; they cannot be annealed out, as in typical liquid crystalline or crystalline structures. We propose below a simple model of these defects and their energies, and demonstrate how their interactions lead to a specific size of condensate.

MODEL

We consider a torus, shown in Fig. 1—which is characterized by the two radii, b and R —formed from one chain (aggregation number, $m = 1$) of length N , to be equivalent to a torus formed from m molecules of length N/m , which are joined end to end such that the joined chains are equivalent to a single chain. The interaxial distance (or the monomer length), d , is typically 25–30 Å (Maniatis et al., 1974). For convenience, we will refer to the torus as being made up of an “ N -length” chain of volume $V \approx b^2 R \approx Nd^3$ for all cases (i.e., all m 's). (Here and henceforth we drop numerical factors (2, π , etc.) of order unity, thereby replacing $=$ with \approx in the corresponding equations.) Accordingly, our theory for preferred size refers to a special value of the total number of monomers, $N (= m \cdot (N/m))$, and not to the chain aggregation number, m .

Imagine a chain of N monomers (each of volume $\approx d^3$) that wraps around itself in an organized manner to make a compact structure, specifically a torus (see Fig. 1), because of some effective interstrand attraction. This attraction can be due to electrostatics (Grønbech-Jensen et al., 1997, Rouzina and Bloomfield, 1996, Oosawa, 1968, and Ray and Manning, 1997) in the multivalent cation-induced condensation, or to depletion interactions in Ψ -condensation (Israelachvili, 1992). Because the size appears to be independent of the condensing agent used, as mentioned in the Introduction, we merely require attraction between the DNA strands and do not examine the nature of the effective attraction. We assume circumferential winding and strand preference for parallel configuration.

The “ N -length” chain forms $\approx b^2/d^2 (=V/Rd^2)$ loops (winds) with average radius R . Each loop is parallel to the other loops, except in the region where it crosses over itself (see Fig. 2 A). The ends of the strands (which will make up other loops) in Fig. 2 A will continue around and eventually be parallel to the noncrossover part of the loop. (Note that whenever “strands” are mentioned, they are part of a loop,

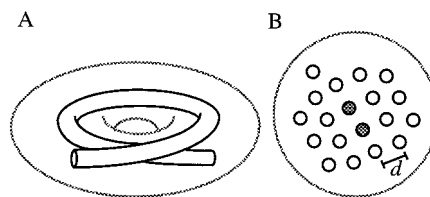


FIGURE 2 (A) A loop within a torus. (B) Cross-sectional view within the torus, where the dark circles represent a crossover pair of strands; d is the interaxial distance. Note the local disruption of hexagonal order.

and do not connote a different chain.) But these crossovers disrupt the hexagonal packing (see Fig. 2 *B*) and introduce local curvature. They are not unlike the twist defects in the hexagonal phases of polymeric liquid crystals (Selinger and Bruinsma, 1992), but here the strands around the crossover respond as if to a splay-type defect. Hence we are not considering a localized chain exchange, but a non-localized “twist” which affects every other strand in its vicinity. We model the crossovers as hard-core inserts imbedded within perfectly packed strands (see Fig. 3 *A* for a 2D representation). We emphasize that these defects are simply convenient models of the crossovers; both crossovers and inserts impose extra local curvature cost and cohesive energy loss.

It may be helpful to note here that, for the remainder of this paper, we will use R and $V^{1/3}$ as the two length scale variables for the torus. The shape of the torus is defined, at fixed volume V , by R , in particular by the ratio $b/R \approx (V/R)^{1/2}/R \approx (V/R^3)^{1/2}$. Large ratios of V/R^3 correspond to a “fat” torus, and small ratios to a “thin” one. A third length scale specifies the defect structure and is defined below.

Because the strands are persistent chains rather than simple particles, there is a “slack” length scale, l (see Fig. 3), over which the chains relax to their parallel configuration. This length corresponds to the extent of the crossover in the real defect. In other words, l is small if the crossover is abrupt, and large if it is very gradual. Small l corresponds to high local curvature and small cohesion loss, and conversely, large l corresponds to small local curvature and large cohesion loss.

We separate the total energy into two components: 1) defect-free, or ideal, and 2) defect energies. The two fundamental physical quantities involved are the cohesion energy density, B/d (\equiv force per unit area), and the bending energy constant, K ($\equiv l_p k_B T$, where l_p is the persistence length of the chain). We shall see that the relative magnitude of these two quantities—in particular, the dimensionless ratio, Bd^3/K —determines the defect slack length (defect “structure”), l^* ; the toroidal shape, R^* ; and ultimately, the preferred size, V^* .

Ideal (defect-free) energy

The volume of the torus is $V \approx b^2 R$, and the surface area $A \approx bR$ ($\approx (V/R)^{1/2} \cdot R \approx (V/R^3)^{1/2}$). Using R as the average radius of curvature for the loops, the energy of the torus

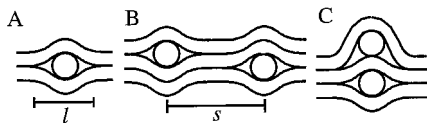


FIGURE 3 Two-dimensional illustration of long-range effect of defects. (A) One defect. (B) Two noninteracting defects. (C) Two interacting defects. The slack length, l , and defect size, a , are shown schematically. In B, the defects are noninteracting (i.e., $s > l$), whereas in C, they are interacting (i.e., $s < l$).

without defects is as follows:

$$E_{\text{defect-free}} \approx -\frac{B}{d}V + BV^{1/2}R^{1/2} + K\frac{(V/d^2)}{R^2}. \quad (1)$$

The first two terms are the cohesive energy contributions (bulk and surface), and the last term is the bending energy contribution to the ideal energy. Here, V/d^2 is the total length of strand bent with an average curvature of $1/R$.

A preferred shape of the torus (i.e., the ratio $b/R \approx (V/R^3)^{1/2}$) for a given volume can be obtained through a minimization of Eq. 1 with respect to R , giving $R_{\text{ideal}}^* \propto V^{1/5}$ (Ubbink and Odijk, 1995; Grosberg and Zhestkov, 1986; Vasilevskaya et al., 1997). Without including the effects of defects, however, Eq. 1 is insufficient for determining a preferred volume.

Defect energy

There are four contributions to the free energy of defects: 1) defect elastic energy, 2) defect-defect interaction energy, 3) loss of cohesion between the strands due to the presence of defects, and 4) defect entropy. Each contribution will be explained separately below.

1. The defect elastic energy is approximated using linear elasticity theory. As explained below, all strands in the cross-sectional area of the defect pay an extra elastic energy cost along the slack length, l (see Fig. 3 *B*). The torus can be divided into $\approx R/l$ l -length “columns” (see Fig. 4), from which follows the number of defects per column, $\rho \approx [(V/Rd^2)/(R/l)] \approx Vl/R^2d^2$. When the defects are far from one another, i.e., defect average center-to-center distance $s \geq l$, the defects are noninteracting ($\rho \leq 1$), and the number of l -length loop portions bent around one defect with curvature κ is $\approx (V/Rd^2)$. Fig. 3 *B* schematically illustrates this point: all of the loop portions (of which only three are shown) around one defect are bent and therefore, the total number of l -length bent loop portions is (number of loops) \times (number of defects) or (number of loops)². The curvature, κ , is $\approx d/l^2$ (see Appendix A1). The defect elastic energy is therefore

$$E_{\text{elas}} \approx K\left(\frac{V}{Rd^2}\right)^2\left(\frac{d}{l^2}\right)^2 l \quad (2)$$

The above energy is positive, and is quadratic in the number of defects. This nontrivial dependence on *size* and *shape* of the torus is a result of the fact that the deformation of strands (loop portions) extends throughout the entire cross

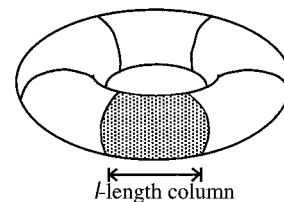


FIGURE 4 Schematic of $2\pi R/l$ “columns” ($= 6$ in the above torus).

section of the torus. More explicitly, the strands relax only through l and not in the plane of the cross-sectional area. This is truly an anisotropic system, and the usual description of defects in an isotropic elastic continuum (Eshelby, 1958) is inapplicable. Therefore, even in the absence of defect-defect interactions, Eq. 2 resembles a two-body effective repulsion between the defects with $1/l^3$ dependence. If $s = l$, the intercolumn distance is exactly l , and the columns do “effectively” interact via a $1/l^3$ dependence. In other words, there is an “intercolumn” (see Fig. 4) interaction that is repulsive.

2. The defect-defect interaction energy is the excess elastic energy cost associated with overlap of defect regions, i.e., where $s < l$ (more than one defect per column), i.e., where $s < l$ (more than one defect per column). If there are R/l “columns” (see Fig. 4), then an average κ^2 can be roughly calculated for a given number of defects per column, ρ . More explicitly, using the $s = 0$ estimate whenever $s < l$ (see Fig. 3 C), a discretized approximation of average κ^2 can be calculated (see Appendix A2). This picture corresponds to noninteracting defects when $s \geq l$, and strongly interacting defects when $s < l$. The average κ^2 can then be used to calculate the elastic energy with defect interactions for a given value of ρ (number of defects per column). When Eq. 2 is subtracted from this elastic energy, which includes defect-defect interactions, we obtain the following crude estimate of the defect interaction energy (see Appendix A2):

$$E_{\text{int}} = 0; \quad l \leq \frac{R^2 d^2}{V} \quad (\rho \leq 1) \quad (3a)$$

$$\approx \frac{Kd^2}{l^3} \left(\frac{V}{Rd^2} \right)^2 \left[\frac{Vl}{R^2 d^2} - 1 \right]; \quad l > \frac{R^2 d^2}{V} \quad (\rho > 1) \quad (3b)$$

The first term in Eq. 3b involves the third power of the number of defects. Because of this strong dependence on the number of defects, there is a very large energetic cost to increasing the number of defects within a column. This interaction energy constitutes an additional effective repulsion between the defects.

3. The defect cohesion energy is the loss of cohesion due to the presence of defects. Each defect, of which there are $\approx V/Rd^2$, is associated with the loss of $\approx l d^2$ in cohesion volume. The defect cohesion energy is then (because B/d is the cohesive energy density):

$$E_{\text{coh}} \approx \frac{B}{d} \left(\frac{V}{Rd^2} \right) l d^2 \quad (4)$$

4. Finally, the defect entropy is approximated by counting the number of ways of arranging the defects within the torus. Because each defect has R/l columns available to it and the total number of defects is $\approx V/Rd^2$, the entropic

contribution to the defect free energy is as follows:

$$E_{\text{entropic}} \approx -k_B T \ln \left[\left(\frac{R}{l} \right)^{V/Rd^2} \right] \quad (5)$$

$$\approx -k_B T \left(\frac{V}{Rd^2} \right) \ln \left(\frac{R}{l} \right)$$

Note that each defect is considered independent but distinguishable, because each loop is distinguishable within the torus. The above contribution serves as an effective (entropic) attraction between the defects, because this term lowers the energy when a large number of defects and/or columns are present. Competition between effective repulsions (Eqs. 2 and 3) and the attraction (Eq. 5) between the defects determines the optimum size. Note that Eq. 4 is an isolated defect energy—i.e., a “perfect” defect energy—where the defects do not feel each other. Although it is necessary to consider this term for the optimum slack length, l^* , Eq. 4 will only change the particular value of the optimum size and will not play a role in the competition discussed above.

When the total defect energy is minimized with respect to the defect structure (or slack length), l , the optimum value l^* can be written as a function of V and R . The resulting total energy is then minimized with respect to R , and the preferred shape is obtained as a function of V . For a range of values of the dimensionless ratio Bd^3/K ($5 \times 10^{-5} < Bd^3/K < 10^{-3}$), there is a preferred size, V^* , as well as a preferred shape, R^* , for the torus.

The cohesive energy for DNA can be obtained crudely from Ψ -condensation experiments (Maniatis et al., 1974). The lowest concentration of poly(ethylene oxide), or PEO, which forms toroids is ~ 80 mg/ml for an average molecular weight of 7500. Treating PEO molecules as ideal particles with a radius equal to the radius of gyration of one molecule (≈ 20 Å), the depletion interaction (Israelachvili, 1992) $\approx -2 \times 10^{-3} k_B T$ per (Å^2) for a DNA separation of 8 Å. The unit length d corresponds to ≈ 28 Å, so $B/d \approx 0.06 k_B T/d^3$. Using this value and $K/d \approx 20 k_B T$ ($l_p/d \approx 20$ or $l_p \approx 550$ Å), we obtain an estimate of $Bd^3/K \approx 0.003$, comparable to values in the range specified above.

Plots of the total energy density as a function of V for three values of Bd^3/K are shown in Fig. 5. When the Bd^3/K ratio is smaller than the minimum value (see Fig. 5 A for $Bd^3/K = 5 \times 10^{-5}$), no condensation is possible (i.e., $V^* \approx 0$), and when the ratio is larger than the maximum value (see Fig. 5 C for $Bd^3/K = 10^{-3}$), the finite-size torus becomes the metastable structure (i.e., $V^* \approx \infty$). For a value of the dimensionless ratio within the range discussed in the above paragraph (see Fig. 5 B for $Bd^3/K = 5 \times 10^{-4}$), there is a preferred size; in Fig. 5 B the preferred size is $\approx 15,000 d^3$, corresponding to $\approx 100,000$ bp.

Although a systematic experimental study of toroidal size as a function of varying Bd^3/K would be extremely difficult, there have been some studies in which the sequence dependence of DNA persistent lengths has been probed (Schnell

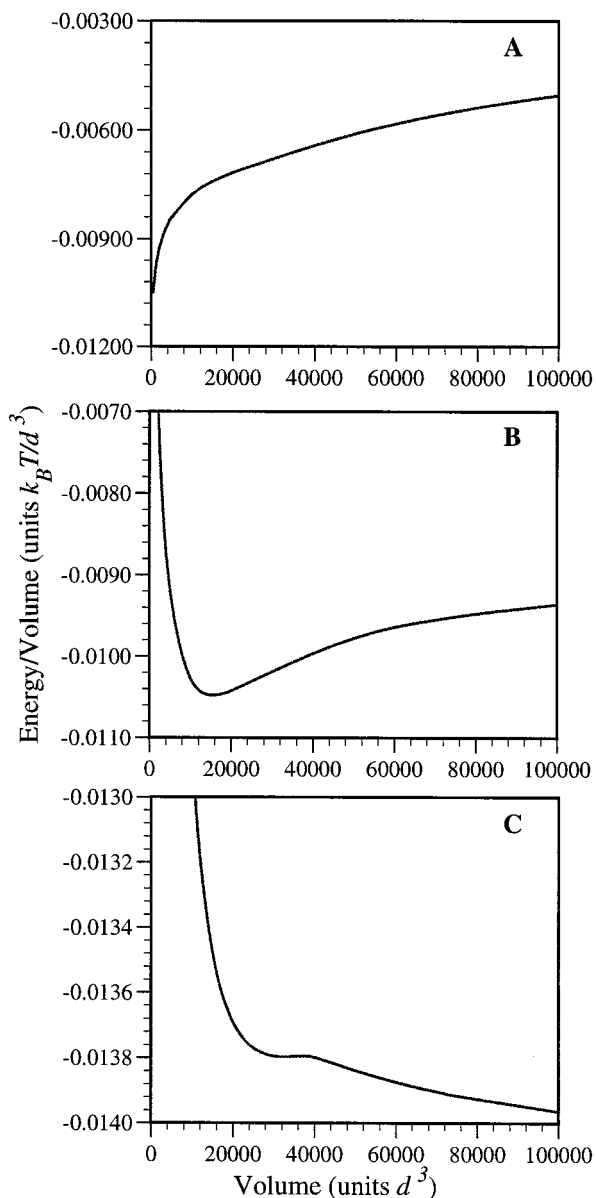


FIGURE 5 Plot of energy per volume (units $k_B T/d^3$) as a function of volume for three values of the dimensionless ratio of cohesive and elastic energies: (A) $Bd^3/K = 5 \times 10^{-5}$. (B) $Bd^3/K = 5 \times 10^{-4}$. (C) $Bd^3/K = 10^{-3}$.

et al., 1998; Reich et al., 1992); the size and shape of the toroidal condensates do vary for nonrandom (i.e., “synthetic”) DNA molecules. For example, Reich et al. (1992) find that some A-T-rich (more flexible) DNA molecules form toroids with much smaller inner radii. It may be worth noting here that we do find a smaller inner toroidal radius with a decrease in the persistence length, and a decrease in the preferred volume with an increase in the persistence length, results not inconsistent with the two studies cited above.

We find that if Bd^3/K is within the stable range, a minimum exists between the noninteracting and interacting defect regimes. Within this range, for volumes smaller than

the minimum value ($V < V^*$), the interaction energy is zero (Eq. 3a), i.e., defects are noninteracting. And for volumes larger than the preferred value ($V > V^*$), the interaction energy is nonnegligible (Eq. 3b), i.e., defects are interacting. This implies that there is a maximum number of noninteracting defects that corresponds to V^* . This maximum number of noninteracting defects determines, then, the preferred size of the toroidal condensates.

DISCUSSION AND REMARKS

We have proposed in this paper that the consistently observed size of DNA condensates is due to the presence of strand crossovers, modeled as hard-core inserts. We show qualitatively that within a range of the dimensionless energy ratio, Bd^3/K , there is a preferred size, as well as a preferred shape, for the toroidal condensates. This size is due to the torus supporting only a certain number of noninteracting defects (or crossovers) for any given V . In liquid crystals or crystals, the macroscopic structure can be annealed so that there is some fixed density of defects. Here, on the other hand, the minimum number of defects is determined purely by the number of loops, or the number of strands in a cross section of the torus. Topologically, there is no way to eliminate these defects within the torus. The only way to achieve an optimum number and density of defects, therefore, is to limit the size of the condensate.

Within the model, the existence of a preferred number of defects in the torus is due to the competition between the defect elastic cost (both the elastic energy and the defect interaction energy) and the defect entropy. The first can be considered as the total “effective” repulsion between the defects, and the second as a defect attraction. When the torus becomes large enough, the repulsive terms—which are quadratic and higher in the number of defects—become dominant over the attractive term—which is roughly linear in the number of defects. Although there is no well-defined range of interaction in the torus, because this is not a true thermodynamic system, e.g., the deformation range is not small compared to the cross-sectional radius b ($\approx (V/Rd^2)^{1/2}$), the above competition is analogous to that between long-range repulsion and the short-range attraction in true bulk systems. For example, condensed domains in Langmuir monolayers are limited in size because the molecules interact via $\sim 1/r^3$ dipolar and $\sim 1/r^6$ dispersive interactions (Andelman et al., 1994). This type of competition has also been studied in nonbulk systems. For example, the shape (cylinder versus necklace) transition of polyelectrolytes—where the number and size of beads can vary (Dobrynin et al., 1996)—is determined by the competition between short-range attraction and the long-range Coulomb repulsion of the charged monomers.

In this paper only the toroidal free energy is examined, i.e., the conformational entropy of the chain is not discussed. The conformational entropy is dependent on the aggregation number (m) and the molecular weight (N/m).

The exact dependence on either of these quantities is not clearly defined. Usually, in monomolecular collapse, a Gaussian coil is assumed in which the confinement entropy (de Gennes, 1979) is approximately $\approx k_B T \cdot R_g^2/R_c^2$ (where $R_g \equiv$ radius of gyration and $R_c \equiv$ radius of confinement). In our present situation, however, the chain within the toroidal condensate is obviously non-Gaussian. Even if we assume a Gaussian chain, the entropy loss is similar to the bending energy cost (see Eq. 1) when the size of confinement is the toroidal radius, R , or equivalently, the volume of the globule is $\approx R^3$. The exclusion of the conformational entropy, then, should not change the qualitative discussion of this model.

Furthermore, we have not included discussion of the size distribution of the toroidal condensates, based on the size dependence of the condensate energy. However, it is clear that if an energetically preferred size exists, there will be a maximum in the size distribution (i.e., an average size should be observable). And the relative depth of the minimum in the intensive energy will determine the width of the distribution, i.e., a shallow well will produce a wide distribution, and a deep one a narrow distribution.

We stress that ours is a qualitative and simple model aimed at addressing the issue of size invariance in the DNA toroidal condensates. The calculations are based on rough estimates of the elastic energy, approximating DNA strands as lines. We have also assumed that the elastic energy can be separated into ideal and defect components. However, the notable feature of this simple model is that topologically unavoidable defects can be responsible for size invariance in these mesoscopic structures.

APPENDIX 1

We approximate here the curvature, κ , for derivation of Eq. 2 of text. If we assume that the contour length of the strand around the defect is $\approx l$, then we only need the curvature dependence on l . The curvature within l will be considered constant for all strands. Then the following geometric argument can be made (see Fig. 6):

$$\begin{aligned} r_c^2 &= (r_c - a)^2 + \left(\frac{1}{2}l\right)^2 \\ r_c &\approx \frac{l^2}{8a}; \quad \text{for } a \ll l/2 \\ \kappa &\equiv \frac{1}{r_c} \approx 8 \frac{a}{l^2} \end{aligned} \quad (\text{A1.1})$$

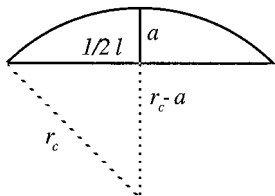


FIGURE 6 Approximation of the curvature for a given height of strand, a , and the length, l .

Here a is used rather than the interaxial spacing, d , for the following reason: the amplitude of the crossover, a , is dependent on the designated mode of winding. There are physical bounds for this value, however, mainly $0 < a < d/2$. The exact value of a does not change the qualitative outcome of the theory. Therefore, we will choose a reasonable value within the physical range. For the choice of $a \approx O(0.1d)$, $\kappa \approx d/l^2$. We use this approximation of the strand curvature.

Because the defect elastic energy is proportional to κ^2 for the length of defect, l , and the number of l -length strands bent with this curvature $\approx (V/Rd^2)^2$,

$$E_{\text{elas}} \approx K \left(\frac{V}{Rd^2}\right)^2 \left(\frac{d}{l^2}\right)^2 l \quad (\text{A1.2})$$

This is Eq. 2 of the text.

APPENDIX 2

A very crude approximation for the defect interaction energy is presented. If ρ ($\approx V/R^2d^2$) is the number of defects ($\approx V/Rd^2$) per column (number of columns $\approx R/l$), the average value of κ^2 for each integral value of ρ can be calculated. Then this discretized calculation of κ^2 versus ρ can be used to approximate the continuous defect interaction energy. The height of the strand, h (see Fig. 6, where $h = a$; also see explanation of a in Appendix 1) increases by $2a$ for each added defect. For $\rho = 2$, for example (see Fig. 7), the average κ^2 is

$$\begin{aligned} \overline{\kappa_{\rho=2}^2} &\approx \frac{\left(\frac{a}{8l^2}\right)^2 + \left(\frac{3a}{8l^2}\right)^2}{2} \\ &\approx \frac{10}{\rho} \kappa_{\text{onedefect}}^2 \end{aligned} \quad (\text{A2.1})$$

Recall that in the case of one defect per column ($\rho = 1$), the curvature is $\approx 8a/l^2$ (cf. Eq. A1.2). The sum of all h^2/a^2 for a given ρ is the coefficient ($1^2 + 3^2 = 10$ in Eq. A2.1). Table 1 shows the general trend of the increase in the coefficients.

The sum of all h^2/a^2 is approximately $\rho^2 (3\rho - 1)/2$. The average curvature for any arbitrary ρ is then

$$\overline{\kappa_{\rho}^2} \approx \frac{\rho^2 (3\rho - 1)}{2\rho} \kappa_{\text{onedefect}}^2 \quad (\text{A2.2})$$

For the elastic energy with overlap, Eq. A2.2 is multiplied by the number of l -length strands bent with this average curvature in the column ($\approx V/Rd^2$) and by the number of columns ($\approx R/l$). This is the defect elastic energy when the defects are interacting. The defect interaction energy is obtained by subtracting from this energy the noninteracting elastic energy (cf. Eq. 2 of text or A1.2). That is, the defect interaction energy is the

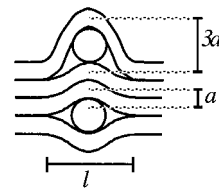


FIGURE 7 Schematic representation of the increase in curvature with each added defect.

TABLE 1 Numerical coefficient for average curvature as function of number of defects per column, ρ

ρ	$\text{sum}(h^2)/a^2$
1	1
2	10
3	35
4	84
5	165

excess elastic energy associated with the overlap of defects:

$$E_{\text{int}} \approx K \left(\frac{V}{Rd^2} \right) \left(\frac{R}{l} \right) \frac{\rho^2(3\rho - 1)}{2\rho} \rho_{\text{onedefect}}^2 l - E_{\text{elas}} \quad (\text{A2.3})$$

$$\approx \frac{Ka^2}{l^3} \left(\frac{V}{Rd^2} \right)^2 [\rho - 1]$$

When $\rho \leq 1$ (when there are just as many or fewer defects than columns—the case of noninteracting defects), Eq. A2.3 is set to 0. This is Eq. 3 of the text.

We are glad to acknowledge Dr. Gary Fujii, who first showed us pictures of DNA condensates and stimulated our interest in this problem. We thank Prof. Avinoam Ben-Shaul for very useful discussions and constructive criticisms throughout the project. We also thank Prof. Robijn Bruinsma and Prof. Joe Rudnick for helpful suggestions and comments.

REFERENCES

- Andelman, D., F. Brochard, C. Knobler, and F. Rondelez. 1994. Structures and phase transitions in Langmuir monolayers. *In* *Micelles, Membranes, Microemulsions, and Monolayers*. W. M. Gelbart, A. Ben-Shaul, and D. Roux, editors. Springer-Verlag, New York. 559–602.
- Ben-Shaul, A., and W. M. Gelbart. 1994. Statistical thermodynamics of amphiphile self-assembly: structure and phase transitions in micellar solutions. *In* *Micelles, Membranes, Microemulsions, and Monolayers*. W. M. Gelbart, A. Ben-Shaul, and D. Roux, editors. Springer-Verlag, New York. 1–104.
- Bloomfield, V. A. 1991. Condensation of DNA by multivalent cations: considerations on mechanism. *Biopolymers*. 31:1471–1481.
- Bloomfield, V. A. 1996. DNA Condensation. *Curr. Opin. Struct. Biol.* 6:334–341.
- de Gennes, P.-G. 1979. *Scaling Concepts in Polymer Physics*. Cornell University Press, Ithaca, NY.
- Dobrynin, A. V., M. Rubinstein, and S. P. Obukhov. 1996. Cascade of transitions of polyelectrolytes in poor solvents. *Macromolecules*. 29:2974–2979.
- Durand, D., J. Doucet, and F. Livolant. 1992. A study of the structure of highly concentrated phases of DNA by x-ray diffraction. *J. Phys. II France*. 2:1769–1783.
- Eshelby, J. D. 1958. The elastic model of lattice defects. *Ann. Physik*. 7:117–121.
- Grønbech-Jensen, N., R. J. Mashl, R. F. Bruinsma, and W. M. Gelbart. 1997. Counterion-induced attraction between rigid polyelectrolytes. *Phys. Rev. Lett.* 78:2477–2480.
- Grosberg, A. Yu., and A. V. Zhestkov. 1986. On the compact form of linear duplex DNA: globular states of the uniform elastic (persistent) macromolecule. *J. Biomol. Struct. Dyn.* 3:859–872.
- Hud, N. V., K. H. Downing, and R. Balhorn. 1995. A constant radius of curvature model for the organization of DNA in toroidal condensates. *Proc. Natl. Acad. Sci. USA*. 92:3581–3585.
- Israelachvili, J. 1992. *Intermolecular and Surface Forces*. Academic Press, San Diego.
- Kornberg, R. D., and Y. Lorch. 1992. Chromatin structure and transcription. *Annu. Rev. Cell Biol.* 8:563–587.
- Laemmli, U. K. 1975. Characterization of DNA condensates induced by poly(ethylene oxide) and polylysine. *Proc. Natl. Acad. Sci. USA*. 72:4288–4292.
- Lepault, J., J. Dubochet, W. Baschong, and E. Kellenberger. 1987. Organization of double-stranded DNA in bacteriophages: a study by cryo-electron microscopy of vitrified samples. *EMBO J.* 6:1507–1512.
- Lerman, L. S. 1974. Chromosomal analogues: long-range order in Ψ -condensed DNA. *Cold Spring Harb. Symp. Quant. Biol.* 38:59–73.
- Lifshitz, I. M., A. Yu. Grosberg, and A. R. Khokhlov. 1978. Some problems of the statistical physics of polymer chains. *Rev. Mod. Phys.* 50:683–713.
- Livolant, F. 1984. Cholesteric organization of DNA in vivo and in vitro. *Eur. J. Cell Biol.* 33:300–311.
- Maniatis, T., J. H. Venable, Jr., and L. S. Lerman. 1974. The structure of Ψ DNA. *J. Mol. Biol.* 84:37–64.
- Manning, G. S. 1980. Thermodynamic stability theory for DNA doughnut shapes induced by charge neutralization. *Biopolymers*. 19:37–59.
- Manning, G. S. 1985. Packaged DNA: an elastic model. *Cell Biophys.* 7:57–89.
- Marx, K. A., and G. C. Ruben. 1983. Evidence for hydrated spermidine-calf thymus DNA toruses organized by circumferential DNA wrapping. *Nucleic Acids Res.* 11:1839–1854.
- Oosawa, F. 1968. Interaction between parallel rodlike macroions. *Biopolymers*. 6:1633–1647.
- Post, C. B., and B. H. Zimm. 1979. Internal condensation of a single DNA molecule. *Biopolymers*. 18:1487–1501.
- Ramakrishnan, V. 1997. Histone structure and the organization of the nucleosome. *Annu. Rev. Biophys. Struct.* 26:83–112.
- Ray, J., and G. S. Manning. 1997. Effect of counterion valence and polymer charge density on the pair potential of two polyions. *Macromolecules*, 30:5739–5744.
- Reich, Z., R. Ghirlando, and A. Minsky. 1992. Nucleic acids packaging processes: effects of adenine tracts and sequence-dependent curvature. *J. Biomol. Struct. Dyn.* 9:1097–1109.
- Rouzina, I., and V. A. Bloomfield. 1996. Macroion attraction due to electrostatic correlation between screening counterions. 1. Mobile surface-adsorbed ions and diffuse ion cloud. *J. Phys. Chem.* 100:9977–9989.
- Schnell, J. R., J. Berman, and V. A. Bloomfield. 1998. Insertion of telomere repeat sequence decreases plasmid DNA condensation by cobalt(III) hexamine. *Biophys. J.* 74:1484–1491.
- Selinger, J., and R. Bruinsma. 1992. Statistical mechanics of defects in polymer liquid crystals. *J. Phys. II France*. 2:1215–1236.
- Ubbink, J., and T. Odijk. 1995. Polymer- and salt-induced toroids of hexagonal DNA. *Biophys. J.* 68:54–61.
- Ubbink, J., and T. Odijk. 1996. Deformation of toroidal DNA condensates under surface stress. *Europhys. Lett.* 33:353–358.
- Vasilevskaya, V. V., A. R. Khokhlov, S. Kidoaki, and K. Yoshikawa. 1997. Structure of collapsed persistent macromolecules: toroid vs. spherical globule. *Biopolymers*. 41:51–60.
- Widom, J., and R. L. Baldwin. 1980. Cation-induced toroidal condensation of DNA: studies with $\text{Co}^{3+}(\text{NH}_3)_6$. *J. Mol. Biol.* 144:431–453.
- Yoshikawa, Y., K. Yoshikawa, and T. Kanbe. 1996. Daunomycin unfolds compactly packed DNA. *Biophys. Chem.* 61:93–100.